Available online at www.sciencedirect.com
SCIENCE DIRECT®
Journal of Magnetism and Magnetic Materials 278 (2004) 39–45
journal of magnetism and magnetic materials
www.elsevier.com/locate/jmmm

X-ray pole figure analysis of sintered PrFeB magnets

A.R.M. Castro, E. Galego, N.B. Lima, R.N. Faria*

Instituto de Pesquisas Energéticas e Nucleares IPEN-CNEN, CEP 05422-970, Sao Paulo, Brazil

Received 15 August 2003; received in revised form 21 October 2003

Abstract

The crystallographic alignment of various permanent magnets has been investigated by X-ray pole figure analysis. The degree of alignment of these sintered magnets has been determined using the (0 0 4) reflection. It has been shown that the (0 0 4) pole figure can be used to measure alignment from a medium to high degree. The degree of alignment, obtained by X-ray diffraction, and the remanence to saturation magnetization ratio have been compared. Attempts have also been made to measure the crystal alignment of permanent magnets using the (1 0 5) X-ray pole figure.

PACS: 71.20.Eh

Keywords: Magnets; Texture; PrFeB-alloys

1. Introduction

It is well known that there is a direct correlation between remanence and texture of permanent magnets. Since the energy product of a magnet is proportional to the square of remanence, a substantial improvement in this magnetic property can be obtained by improving crystallographic alignment. Thus, texture analysis is currently considered as an important tool and several studies to evaluate the degree of crystal alignment of permanent magnets, using X-ray diffraction, have been reported [1–10]. No systematic studies of magnetic alignment in the PrFeB system using the (0 0 4) reflection have been reported so far. In this study, the crystal alignment of $Pr_{16}Fe_{76}B_8$ sintered magnets has been investigated using the (0 0 4) X-ray pole figure analysis. Attempts have also been made to use (1 0 5) X-ray pole figures to quantify the crystallographic alignment of sintered magnets. In this investigation, the ratio of remanence to saturation magnetization (B_r/M_s) has been compared with the results of X-ray diffraction.

2. Experimental

A commercial $Pr_{16}Fe_{76}B_8$ alloy in the as-cast state was used in this study. To produce the sintered Pr-based magnets using the hydrogen decrepitation (HD) process [11], 35 g of the bulk ingot were placed in a stainless steel hydrogenation vessel, which was then evacuated to backing-pump pressure. Hydrogen was introduced to a pressure

*Corresponding author. Tel.: +011-38169345; fax: +011-38169370.
E-mail address: rfaria@net.ipen.br (R.N. Faria).

0304-8853/$ - see front matter © 2003 Elsevier B.V. All rights reserved.
doi:10.1016/j.jmmm.2003.11.371

of 1 bar, which resulted in decrepitation of the bulk material. The standard decrepitated hydride material was then transferred to a "roller" ball-mill under a protective atmosphere and milled for several hours (9, 18, 27, 36 and 45 h) using cyclohexane as the milling medium. The resultant fine powder was then dried for 1 h and transferred to a small cylindrical rubber tube under a nitrogen atmosphere. The fine powder was aligned by pulsing three times to a 6 T magnetic field, pressed isostatically at 1000 kg cm^{-2} and then vacuum sintered for 1 h at 1060°C, followed by cooling on the furnace ($\sim$3.5°C min^{-1}). Heat treatment was carried out under vacuum at 1000°C for 24 h. Magnetic measurements of the HD sintered magnets were performed in a permeameter after saturation in a pulsed field of 6 T.

Although it is possible to vary the degree of alignment in sintered magnets, by changing the intensity of the orientation field [12,13], in this investigation, the milling stage was used to change the degree of grain alignment in the $Pr_{16}Fe_{76}B_8$ magnets. Hydrogen desorption from the powder prior to the milling step was also employed to vary the degree of alignment in these HD $Pr_{16}Fe_{76}B_8$ magnets [14]. Partially desorbed powder was prepared from the decrepitated hydride by a heat treatment in vacuum at 300°C for 5 h. Total desorption of the powder was also carried out in vacuum but at 600°C for 5 h. The partially and totally desorbed material was then processed in the same manner as the standard decrepitated hydride material. The samples, as-sintered and heat treated, were examined by X-ray diffraction techniques. Previous studies [5,15] employed the (0 0 6) pole figure to determine the texture in Nd-based magnets. In this study, preliminary evaluation showed that the (0 0 6) reflection is close to the (3 3 1), (4 0 2) and (3 1 4) reflections, all with strong relative intensities, which could cause overlap in the X-ray pole figure measurements. Therefore, the (0 0 4) reflection was chosen in this investigation. The (1 0 5) X-ray pole figure was investigated because this reflection showed high intensity in all well-aligned magnets. Measurements of (0 0 4) and (1 0 5) pole figures were carried out by the Schulz's reflection method with a diffractometer, using the Cr K_α radiation [1]. The tilt angle (α) was varied from 0° to 75° in steps of 5°. The angle of rotation, azimuth angle (β), was varied from 0° to 360° in steps of 5°. The intensities of the pole figure data were normalized by

$$I(\alpha_j) = \frac{\sum_{i=1}^{72} f(\alpha_j, \beta_i)}{72 I(\alpha_1)} \quad j = 1, 16. \tag{1}$$

The (0 0 4) normalized intensity data was then fitted for a Gaussian distribution, and $\langle \cos \Theta \rangle$ was calculated based on the Stoner–Wohlfarth model [16], using

$$\langle \cos \Theta \rangle = \frac{B_r}{M_s} = \frac{\int_0^{\pi/2} \exp(-\boldsymbol{\alpha}^2/2\boldsymbol{\sigma}^2) \sin \boldsymbol{\alpha} \cos \boldsymbol{\alpha} \, d\boldsymbol{\alpha}}{\int_0^{\pi/2} \exp(-\boldsymbol{\alpha}^2/2\boldsymbol{\sigma}) \sin \boldsymbol{\alpha} \, d\boldsymbol{\alpha}}, \tag{2}$$

where M_s is the saturation magnetization of the magnet, B_r is the remanence of the magnets and α is the angle between the tetragonal c-axis and the applied field [12]. The (1 0 5) normalized intensity data was fitted for two Lorentz functions centered at 0° and 15° from magnet alignment direction and the ratio L_{105} was calculated by

$$L_{105} = \frac{L(\Theta_c = 15^o)}{L(\Theta_c = 0^o)}, \tag{3}$$

$L(\Theta_c = 15°)$ and $L(\Theta_c = 0°)$ are the maximum intensity values of the Lorentz functions.

The saturation magnetization for the $Pr_{16}Fe_{76}B_8$ (wt%: 34.24Pr-64.45Fe-1.31B) magnets was estimated (assuming that all Fe in the magnet exists in the $Pr_2Fe_{14}B$ phase) using the following expression [12]:

$$M_s = M_S^N \frac{W_{Fe} \, W_N^M \rho_s}{100 \, 14 \, W_{Fe}^M \rho_N}, \tag{4}$$

where M_S^N is the saturation magnetization of $Pr_2Fe_{14}B$ at 300 K (1.56 T [17]), W_{Fe} is the weight percentage of Fe in the magnet (64.45%), W_{Fe}^M is the molecular weight of Fe (55.85 g/mol), W_N^M is the molecular weight of $Pr_2Fe_{14}B$ (1074.47 g/mol [18]), ρ_N is the X-ray density of $Pr_2Fe_{14}B$ (7.53 g/cm^3 [19]) and ρ_s is the measured specific density of the sintered magnet. The densities of the permanent magnets were measured using a liquid displacement system.

3. Results and discussion

Fig. 1 shows a two-dimensional (0 0 4) pole figure and a three-dimensional (3D) plot for a sintered magnet with a high degree of crystallographic alignment ($\langle \cos \Theta \rangle = 0.97$). The circular lines, which correspond to changes in the intensity of the (0 0 4) diffraction lines, show a well-defined sharp pattern. Fig. 2 shows the (1 0 5) pole figure and the 3D plot for the same sintered magnet. In this case, some broadening of the contour lines occurred, but without degradation of the pattern. Fig. 3 shows a (0 0 4) pole figure and the 3D plot for a sintered magnet with a lesser degree of crystallographic alignment ($\langle \cos \Theta \rangle = 0.88$). Fig. 4 shows the (1 0 5) pole figure and the 3D plot for the same sintered magnet. In both cases, some broadening of the circular lines occurred with some degradation of the pattern.

Curves for normalized intensities (0 0 4), obtained using Eq. (1) and plotted as a function of α angle for various magnets, are shown in Fig. 5. Magnets with a high degree of alignment showed sharp curves and those with a lesser degree of alignment showed a broadening of the curve profile. Sintered magnets, processed in different manners, but with a high degree of alignment showed (0 0 4) curves with poor resolution and this can be observed in Fig. 6 (the normalized intensities are below zero in the range of $\alpha \approx 30-60^\circ$ due to the background correction statistics). In this case, all magnets showed a degree of alignment of 0.97. Normalized intensities for the reflections (1 0 5) of these magnets, shown in Fig. 7, however, exhibited a maximum at approximately 15° for two magnets ($L_{105} = 0.98$ and 1.07), due to the influence of the [0 0 1] magnetic alignment direction. These gives an indication that these two magnets are slightly better aligned than that which did not show a maximum at low angles.

Figs. 8 and 9 show the measured remanence of the sintered magnets, as a function of $\langle \cos \Theta \rangle$

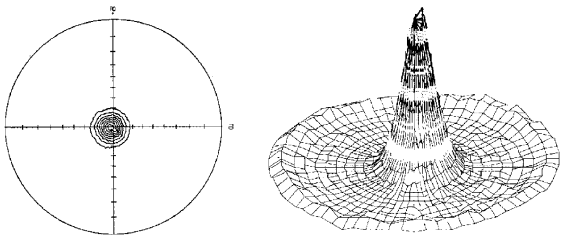

Fig. 1. (0 0 4) pole figure and 3D plot for a sintered magnet with degree of crystallographic alignment of 0.97. Isolines intensity in times random (TR): 2.1, 4.2, 6.4, 8.5, 10.6, 12.7, 14.8, 16.9 and 19.1.

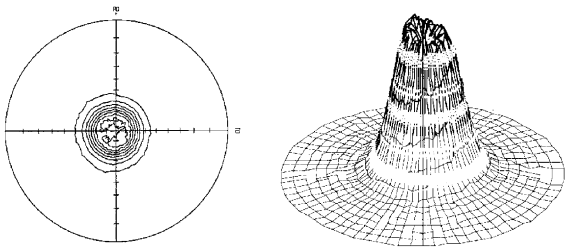

Fig. 2. (1 0 5) pole figure and 3D plot for a sintered magnet with degree of crystallographic alignment of 0.97. Isolines intensity (TR): 0.6, 1.3, 1.9, 2.6, 3.2, 3.8, 4.5, 5.1 and 5.7.

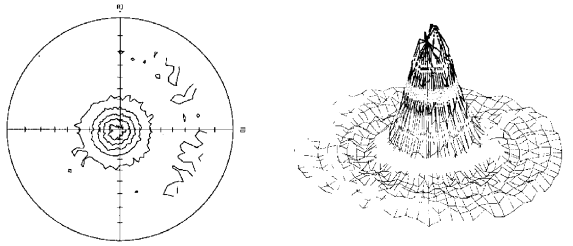

Fig. 3. (0 0 4) pole figure and 3D plot for a sintered magnet with degree of crystallographic alignment of 0.88. Isolines intensity (TR): 0.9, 1.7, 2.6, 3.4 and 4.3.

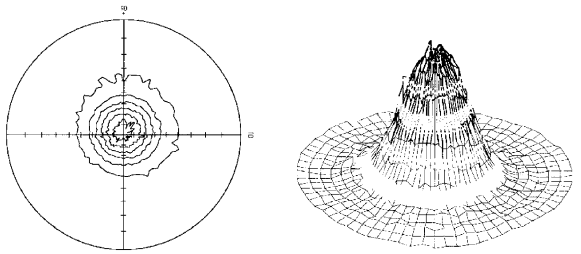

Fig. 4. (1 0 5) pole figure and 3D plot for a magnet with degree of crystallographic alignment of 0.88. Isolines intensity (TR):0.7, 1.3, 2.0, 2.7, 3.3 and 4.0.

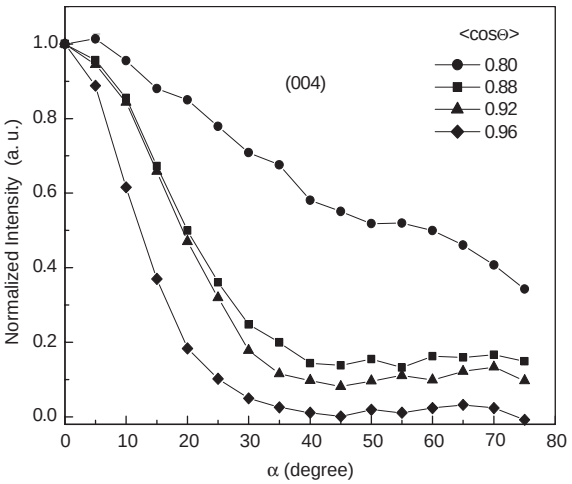

Fig. 5. Normalized intensities as a function of angle α for four magnets (as-sintered condition) with distinct degrees of alignment, for the reflections (0 0 4).

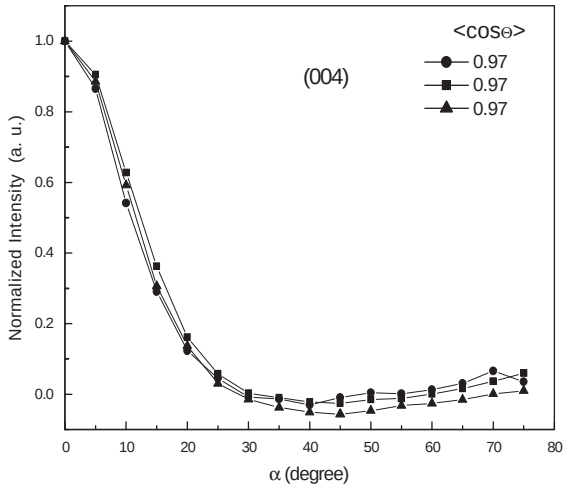

Fig. 6. Normalized intensities as a function of angle α for three heat-treated magnets with high degrees of alignment, for the reflections (0 0 4).

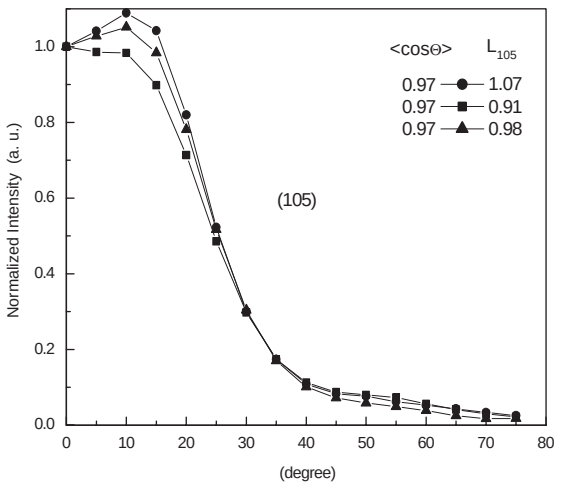

Fig. 7. Normalized intensities as a function of angle α for three heat-treated magnets with high degrees of alignment, for the reflections (1 0 5).

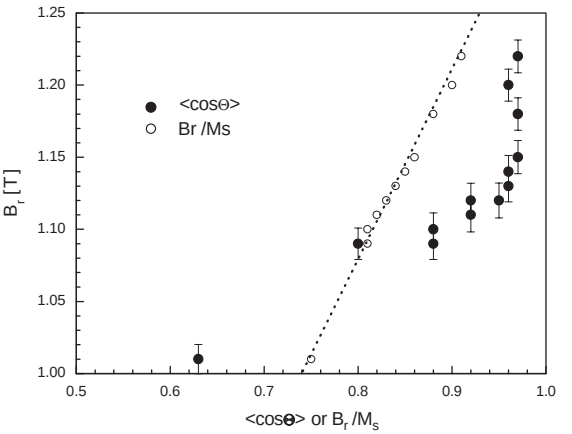

Fig. 8. Variation of remanence of sintered magnets with degree of alignment.

and L_{105}, respectively. The ratio B_r/M_s was also plotted for comparison, since this ratio is often used as the degree of alignment in permanent magnets. It can be seen that $\langle \cos \Theta \rangle$ is a good parameter for samples that exhibit degrees of orientation up to 0.95, but is not a very sensitive parameter for magnets that exhibit higher degrees of orientation. L_{105}, on the other hand, is more sensitive in the case of magnets with a high degree of orientation but it showed a wide scatter and no meaningful conclusion could be drawn. Theoretically, the index L_{105} ranges from 0 to ∞, that is, from minimum to maximum alignment of the "c" axis with the magnetic field. The $\langle \cos \Theta \rangle$ obtained by pole figure analysis was found to be less sensitive at high degrees of alignment because of the $I(\alpha)$ broadening. The instrumental profile is very broad in the Schulz's method. Besides,

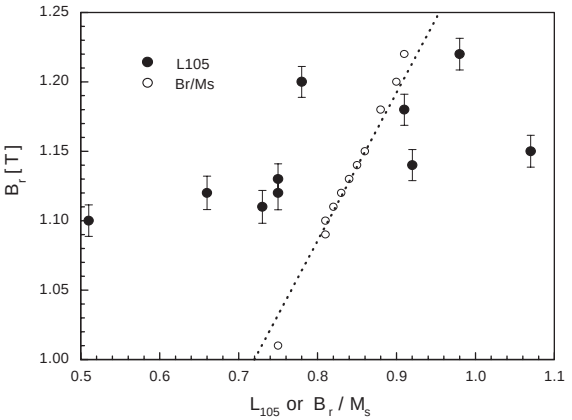

Fig. 9. Variation of remanence of sintered magnets with L_{105}.

defocusing effects and other geometrical imperfections also occur. For low degrees of alignment, the $I(\alpha)$ is influenced by the neighboring diffraction peaks. The size of the magnet's cystallites also causes $I(\alpha)$ broadening.

The remanence of a permanent magnet depends directly on the volume fraction (f) and saturation polarization (M_s) of the hard magnetic phase (ϕ), as well as on the degree of easy-axis alignment of the single crystals ϕ grains ($\langle \cos \Theta \rangle$) and magnet density. The remanence can be estimated from the expression [20,21]:

$$B_r = \langle \cos \Theta \rangle f P M_s. \quad (5)$$

The degree of alignment is 0.5 for an isotropic magnet and increases to 1 for a perfectly aligned magnet. Good sintered magnets should have $\langle \cos \Theta \rangle$ around 0.92–0.95 [14]. The volume fraction ($0 \leqslant f \leqslant 1$) of the matrix phase in an ideal magnet is unity, but to achieve high densification, sintered magnets are produced with higher amounts of rare earth, usually around 0.82–0.85. The ratio of magnet density to theoretical density (P) for an ideal magnet is unity, and in sintered magnets it can reach 0.96 [14]. The method used in the present work to change the degree of alignment also affects the volume fraction of the matrix phase. This could help to explain the remanence behavior shown in Fig. 8. Changing the degree of alignment by varying the orientating magnetic field during powder compaction should not affect P and f, but it has been shown that these parameters have a non-linear relationship [12,13].

Table 1 gives a summary of the degree of alignment, remanence, intrinsic coercivity, squareness factor, density, spontaneous magnetization and processing conditions for all magnets studied in this investigation. The two magnets that showed a maximum of the normalized intensity at $\alpha \approx 15^\circ$ ($L_{105} = 0.98$ and 1.07; Fig. 7) are slightly better aligned than the one that did not show a maximum at low angles and this is in contrast to Table 1. The highest value for the normalized intensity at $\alpha \approx 15^\circ$ was obtained for the magnet with $\langle \cos \Theta \rangle = 0.97$ and $L_{105} = 1.07$. This magnet, however, shows the lowest B_r- and B_r/M_s-values of the magnets with $\langle \cos \Theta \rangle = 0.97$. This is due to the processing conditions for this particular magnet. In this case, the HD material was milled for 45 h and this overmilling decreased the volume fraction (f) of the matrix phase. Thus, although the crystal alignment is slightly superior in this sintered magnet the remanence is somewhat inferior due to the lower amount of the $Pr_2Fe_{14}B$ phase and the slightly reduced density. Overmilling increases alignment but also causes the oxidation of the magnetic powder [14].

Values of degree of crystallographic alignment determined by (0 0 4) pole figures are suitable for use in Eq. (5). This was not the case for previously reported degree of crystallographic alignment in permanent magnets [12,22] (it is also clear that the values of the index L_{105} could not be used in this equation since it can be higher than unity). It is also appropriate to mention that previous attempts to correlate the degree of alignment and squareness factor ($SF = 4(BH)_{max}/B_r^2$) for Sm-Co magnets showed a wide scatter and no meaningful conclusions could be drawn [23]. Although, $\langle \cos \Theta \rangle$ and squareness factor ($SF = H_k/_i H_c$) seem to have a correlation in Pr-based sintered magnets [14], these parameters are measures of different properties. The former is a true measure of the degree of alignment of the magnet, whereas the latter is a measure of the amount of magnetic grains that reversed its magnetization for a determined demagnetization field. Even though all techniques for measurement of crystallographic alignment have some limitations, as pointed out by

Table 1
Degree of alignment, magnetic properties, density, spontaneous magnetization and processing conditions of $Pr_{16}Fe_{76}B_8$ sintered magnets

$\langle \cos\Theta \rangle$ (±1%)	B_r (T) (±1%)	SF ($=H_k/_iH_c$) (±2%)	$\mu_i H_c$ (T) (±2%)	ρ_s (g/cc) (±0.3%)	$M_s = 0.183\ \rho_s$(T)	B_r/M_s	L_{105} (±1%)	Milling time (h), powder and magnet condition[a]
0.63	1.01	0.62	1.36	7.30	1.34	0.75	—	9-HD-A
0.80	1.09	0.77	1.49	7.37	1.35	0.81	—	18-HD-A
0.88	1.09	0.81	1.75	7.38	1.35	0.81	—	18-HD-H
0.88	1.10	0.79	1.32	7.38	1.35	0.81	0.51	27-HD-A
0.92	1.11	0.75	1.43	7.35	1.35	0.82	0.73	36-HD-A
0.92	1.12	0.89	1.67	7.39	1.35	0.83	0.66	27-HD-H
0.95	1.12	0.81	1.53	7.37	1.35	0.83	0.75	36-HD-H
0.96	1.13	0.66	1.45	7.33	1.34	0.84	0.75	18-PD-A
0.96	1.14	0.84	1.39	7.32	1.34	0.85	0.92	45-HD-A
0.96	1.20	0.73	0.99	7.33	1.34	0.90	0.78	18-TD-A
0.97	1.18	0.93	1.52	7.33	1.34	0.88	0.91	18-PD-H
0.97	1.22	0.79	1.06	7.33	1.34	0.91	0.98	18-TD-H
0.97	1.15	0.93	1.49	7.30	1.34	0.86	1.07	45-HD-H

[a] HD: hydrogen decrepitated, PD: partially degassed, TD: totally degassed, A: as-sintered state, H: heat treated.

Lewis et al. [10], pole figure analysis has the advantage of yielding an index ($\langle \cos\Theta \rangle$) that can be used in mathematical expressions for more precise quantification of the magnet's parameters.

4. Conclusions

The index $\langle \cos\Theta \rangle$, determined by the (0 0 4) pole figure analysis, is a good index to represent the degree of alignment of sintered permanent magnets. The alignment index provided by this method is convenient for use in mathematical equations and for general use in quantitative calculations of remanence values. In magnets with a high degree of crystallographic alignment, the index L_{105} could be employed to verify small differences in texture. Remanence is useful to compare the degree of alignment of sintered permanent magnets provided that the volume fraction of the matrix phase and density remain constant in all magnets under comparison.

Acknowledgements

Many thanks are due to FAPESP and IPEN-CNEN for supporting this investigation. Thanks are also due to M.M. Serna and K. Imakuma for their help during the course of this work.

References

[1] L.G. Schulz, J. Appl. Phys. 20 (1949) 1030.
[2] J.F. Herbst, J.C. Tracy, J. Appl. Phys. 50 (6) (1979) 4283.
[3] K.D. Durst, H. Kronmuller, J. Magn. Magn. Mater. 59 (1986) 86.
[4] W.C. Chang, T.B. Wu, K.S. Liu, J. Appl. Phys. 63 (8) (1988) 3531.
[5] S.Z. Zhou, Y.X. Zhou, C.D. Graham Jr., J. Appl. Phys. 63 (8) (1988) 3534.
[6] A.S. Kim, F.E. Camp, H.H. Stadelmaier, J. Appl. Phys. 76 (10) (1994) 6265.
[7] Y. Kaneko, N. Ishigaki, J. Mat. Eng. Perform. 3 (2) (1994) 228.
[8] D. Hinz, S. Wirth, D. Eckert, K. Helming, K.H. Muller, J. Magn. Magn. Mater. 157 (1996) 43.
[9] Y.R. Wang, S. Guruswamy, J. Appl. Phys. 81 (8) (1997) 4450.
[10] L.H. Lewis, T.R. Thurston, V. Panchanathan, U. Wildgruber, D.O. Welch, J. Appl. Phys. 82 (7) (1997) 3430.
[11] R.N. Faria, A.J. Williams, J.S. Abell, I.R. Harris, Proceedings of the 14th International Workshop on RE Magnets and Applications, São Paulo, 1996, p. 570.
[12] T. Kawai, B.M. Ma, S.G. Sankar, W.E. Wallace, J. Appl. Phys. 67 (9) (1990) 4610.
[13] P.J. McGuiness, I.R. Harris, E. Rozendaal, J. Ormerod, M. Ward, J. Mater. Sci. 21 (1986) 21.

[14] R.N. Faria, A.R.M. Castro, N.B. Lima, J. Magn. Magn. Mater. 238 (2002) 38.
[15] W.C. Chang, T.B. Wu, K.S. Liu, J. Magn. Magn. Mater. 78 (1989) 283.
[16] E.C. Stoner, E.P. Wohlfarth, Philos. Trans. R. Soc. London 240 (1948) 599.
[17] S. Hirosawa, Y. Matsuura, H. Yamamoto, S. Fujimura, M. Sagawa, J. Magn. Magn. Mater. 59 (3) (1986) 873.
[18] R.N. Faria, J. Magn. Magn. Mater. 238 (2002) 56.
[19] M. Jurczyk, O.D. Cristjakov, J. Magn. Magn. Mater. 78 (1989) 279.
[20] R.A. McCurrie, J. Appl. Phys. 52 (12) (1981) 7344.
[21] C.W. Searle, V. Davis, R.D. Hutchens, J. Appl. Phys. 53 (3) (1982) 2395.
[22] N.B. Lima, M.M. Serna, H.O. Santos, R.N. Faria, A.J. Williams, I.R. Harris, Proceedings of the 8th International Symposium on Magnetic Anisotropy and Coercivity in RE Transactions of Metal Alloys, Birmingham, 1994, p 109.
[23] D.L. Martin, H.F. Mildrum, S.R. Trout, Proceedings of the 8th International Workshop on RE Magnets and Applications, Dayton, 1985, p. 269.